2006

Application of Relative Drought Indices in Assessing Climate-Change Impacts on Drought Conditions in Czechia

M. Dubrovsky
Institute of Atmospheric Physics, Academy of Sciences CR, Bocni II/1401, 14131 Prague, Czechia

Mark D. Svoboda
University of Nebraska - Lincoln, msvoboda2@unl.edu

M. Trnka
Institute for Agrosystems and Bioclimatology, Mendel University of Agriculture and Forestry, Zemedelska 1, 61300 Brno, Czechia

Michael J. Hayes
University of Nebraska-Lincoln, mhayes2@unl.edu

Donald A. Wilhite
University of Nebraska - Lincoln, dwilhite2@unl.edu

See next page for additional authors

Authors
M. Dubrovsky, Mark D. Svoboda, M. Trnka, Michael J. Hayes, Donald A. Wilhite, Z. Zalud, and P. Hlavinka

Published in *Theoretical and Applied Climatology* 96 (2009), pp. 155–171; doi: 10.1007/s00704-008-0020-x.

Submitted November 14, 2006; accepted January 11, 2008; published online April 29, 2008.

Application of Relative Drought Indices in Assessing Climate-Change Impacts on Drought Conditions in Czechia

M. Dubrovsky,[1] M. D. Svoboda,[2] M. Trnka,[3] M. J. Hayes,[2] D. A. Wilhite,[2] Z. Zalud,[3] and P. Hlavinka[3]

1. Institute of Atmospheric Physics, Academy of Sciences CR, Bocni II/1401, 14131 Prague, Czechia
2. National Drought Mitigation Center, University of Nebraska, 815 Hardin Hall, Lincoln, NE 68583, USA
3. Institute for Agrosystems and Bioclimatology, Mendel University of Agriculture and Forestry, Zemedelska 1, 61300 Brno, Czechia

Corresponding author – M. Dubrovsky, Hodesovice 119, 53322 Byst, Czechia, email dub@ufa.cas.cz

Abstract

The common versions (referred to as self-calibrated here) of the Standardized Precipitation Index (SPI) and the Palmer Drought Severity Index (PDSI) are calibrated and then applied to the same weather series. Therefore, the distribution of the index values is about the same for any weather series. We introduce here the relative SPI and PDSI, abbreviated as rSPI and rPDSI. These are calibrated using a reference weather series as a first step, which is then applied to the tested series. The reference series may result from either a different station to allow for the interstation comparison or from a different period to allow for climate-change impact assessments. The PDSI and 1–24 month aggregations of the SPI are used here. In the first part, the relationships between the self-calibrated and relative indices are studied. The relative drought indices are then used to assess drought conditions for 45 Czech stations under present (1961–2000) and future (2060–2099) climates. In the present climate experiment, the drought indices are calibrated by using the reference station weather series. Of all drought indices, the PDSI exhibits the widest spectrum of drought conditions across Czechia, in part because it depends not only on precipitation (as does the SPI) but also on temperature. In our climate-change impact experiments, the future climate is represented by modifying the observed series according to scenarios based on five Global Climate Models (GCMs). Changes in the SPI-based drought risk closely follow the modeled changes in precipitation, which is predicted to decrease in summer and increase in both winter and spring. Changes in the PDSI indicate an increased drought risk at all stations under all climate-change scenarios, which relates to temperature increases predicted by all of the GCMs throughout the whole year. As drought depends on both precipitation and temperature, we conclude that the PDSI is more appropriate (when compared to the SPI) for use in assessing the potential impact of climate change on future droughts.

1. Introduction

Droughts are considered to be amongst the cumulative climate hazards (Oliver 2005). Generally, drought originates from a deficiency of precipitation over an extended period of time, usually a season or more. Drought is a slow-onset disaster and its effects often accumulate slowly over a considerable period of time. Drought affects many regions of the world and is the costliest climatic hazard globally (Wilhite 2000). As a result, some of the affected countries pay a great deal of attention to this phenomenon and employ various tools for monitoring and forecasting it (e.g., U.S. Drought Monitor, located at http://www .drought.unl. edu/dm/monitor.html, Svoboda et al. 2002).

In assessing recent changes in climate and projected climate change for the forthcoming decades, the 3rd IPCC report on climate change (Houghton et al. 2001) states that increased summer drying over most midlatitude continental interiors and the associated risk of drought was likely in the 20th century (based on observations) and is assumed to continue into the 21st century [based on Global Climate Model (GCM) simulations]. This drying is expected to have many undesirable effects such as decreased crop yields, increased damage to building foundations caused by ground shrinkage, decreased water resource quantity and quality, and increased risk of forest fire (McCarthy et al. 2001).

An increasing trend in drought is indicated in studies made by Brunetti et al. (2002; Italy), Bonaccorso et al. (2003; Sicily), Piccarreta et al. (2004; southern Italy), Watson et al. (1997; Mediterranean region), Vicente-Serrano et al. (2004; eastern Spain), Smith et al. (1996; central Europe), and Trnka et al. (2008; Czechia). Dai et al. (2004) found that the very dry areas (defined in terms of the PDSI) around the globe have more than doubled since the 1970s. On the other hand, Lloyd-Hughes and Saunders (2002), who developed a drought climatology for Europe, found only insignificant changes in extreme and/or moderate drought conditions during the 20th century. A similar outcome was obtained by van der Schrier et al. (2006), who used the self-calibrated PDSI (see below for an explanation) and found that trends in summer soil moisture availability over Europe for the 1901–2002 period fail to be statistically significant, both in terms of spatial means of the drought index and in the area affected by the drought. Based on analysis of 600 daily streamflow records from Europe, Hisdal et al. (2001) claims that it is not possible to conclude that drought conditions in general have become more severe or frequent. Although no significant changes were detected for most stations, they found distinct regional differences for 1962–1990 trends: drought deficit volumes increased in Spain, eastern Central Europe (including Czechia and Slovakia), and large parts of the United Kingdom, but decreased in Eastern Europe and Central Europe. They admit that the changes may be partly due to artificial influences in the catchments.

With projected global temperature increases, it is generally agreed upon that the global hydrological cycle will intensify and the extremes will become, or have already become, more common (Hisdal et al. 2001). The recent GCM-based projections of the future climate suggest significant changes in temperature and precipitation patterns (Houghton et al. 2001). For large regions of the world, the models predict an increase in temperature coupled with a precipitation decrease, which will lead to further increases in drought risk in those regions. Specifically, considering the projected increases in temperature over Central Europe along with a slight gain in precipitation amounts in both the winter and spring months (and decreases in summer months) (Dubrovský et al. 2005), it is very likely that the frequency of drought occurrence and its severity will increase in Central Europe and the impacts associated with these events will be exacerbated. Jones et al. (1996; cited by Vicente-Serrano et al. 2004) predicted that by the end of the 21st century, Europe will face increases in the intensity, duration, and spatial extent of drought in the Mediterranean basin.

There exists no precise definition for drought, and any such definition should be based on particular needs, which are sector- and region-specific. Generally, four types of drought are recognized (Heim 2002): (1) meteorological drought; (2) agricultural drought; (3) hydrological drought; and (4) socioeconomic drought. Meteorological drought usually relates to the departure of precipitation from its normal over some period of time. Agricultural drought also accounts for soil moisture, and hydrological drought typically covers water resources (supply) in the form of streamflows, groundwater, and reservoir levels. Socioeconomic drought is associated with the supply and demand of some economic good, with elements of the three previous types of drought.

Numerous drought indices have been developed to characterize drought (for reviews, see, e.g., Keyantash and Dracup 2002; Heim 2002). Of these, the most common indices used worldwide include the *Standardized Precipitation Index* (SPI) (developed by McKee et al. 1993) and the *Palmer Drought Severity Index* (PDSI), developed by Palmer (1965). Complete descriptions of the equations can also be found in Alley (1984).

The Standardized Precipitation Index is the transformation of the precipitation amount aggregated over a selected period (commonly 1 to 24 months) into a standardized normal distribution. It has been used in many studies (e.g., Lana et al. 2001; Hayes et al. 1999; Seiler et al. 2002; Vicente-Serrano et al. 2004; Rouault and Richard 2003) and has become an important component in many drought-monitoring efforts (i.e., the U.S. Drought Monitor, located at http://drought.unl.edu/dm, and the North American Drought Monitor, located at http://www.ncdc.noaa.gov/oa/ climate/monitoring/drought/nadm). A May–July SPI series for Turkey was reconstructed from tree rings by Touchan et al. (2005) for the 1251–1998 period and then used to analyze dry and wet events. Lloyd-Hughes and Saunders (2002) developed a high spatial resolution, multitemporal SPI-based climatology of Europe; they also pointed out advantages and disadvantages of this index. SPI maps are operationally available for the U.S.A. at http://www. drought.unl.edu/monitor/spi.htm.

While the SPI is based solely on precipitation, the PDSI requires temperature and characteristics of the soil, in addition to precipitation, for a generic two-layer soil water balance model. Despite its many limitations (described in detail by Alley 1984, and Karl and Knight 1985), including frequent criticism for the complexity and untransparency of the index, the

PDSI has become one of the most widely used drought-assessment tools (Byun and Wilhite 1999; Szalai and Szinell 2000; Szinell et al. 1998; Zou et al. 2005). Dai et al. (2004) derived a global gridded monthly PDSI dataset for 1870–2002 and found that the PDSI is a good proxy for both surface moisture conditions and streamflow. Wells et al. (2004) introduced the self-calibrated PDSI (scPDSI), in which the empirical constants of the computational algorithm are replaced with values dynamically calculated from the local input weather series (in contrast with the original algorithm, in which the constants are based on a small number of stations from different climates). This modification affects the distribution of the index values, so that it falls bellow −4 with about 2% probability as well as exceeds +4 with 2% probability. Van der Schrier et al. (2006) derived the time series (1901–2002) and maps of scPDSI for Europe from the gridded temperature and precipitation data (0.5° × 0.5° resolution) compiled by the Climate Research Unit (Mitchell and Jones 2005). Historical PDSI maps for the conterminous U.S. are available on the web at http://www.drought.unl.edu/whatis/palmer/pdsihist.htm. Historical PDSI time series were reconstructed from tree rings by Woodhouse and Brown (2001) for eastern Colorado and then used for historical drought assessments (Woodhouse et al. 2002).

Depending on the time scale of the SPI, this index may be closely correlated with the PDSI. Lloyd-Hughes and Saunders (2002) found that the correlation between SPI and PDSI reaches a maximum (0.73) using a 9- to 12-month aggregation. Similarly, Redmond (2002) found a high correlation of PDSI with SPI aggregated over 6 to 12 months. Bordi and Sutera (2001; cited by Bonaccorso et al. 2003) have shown that the main patterns of drought variability obtained by using the PDSI and 24-month SPI compare favorably.

The values of SPI and PDSI may be converted into drought categories that express drought severity with respect to normal conditions at a given site. For the SPI, the categories span from extremely dry (SPI ≤ −2) to extremely wet (SPI ≥ 2), with normal falling within (−1, +1) (http:// www.drought.unl.edu/whatis/indices.htm). For the PDSI, the categories go from extreme drought (PDSI ≤ −4) to extremely wet (PDSI ≥ 4), with near-normal conditions being indicated by PDSI $\in < -0.5, +0.5 >$ (http://www.drought.unl.edu/whatis/indices.htm).

Drought may also be defined by other characteristics, such as periods with precipitation lower than a given threshold—e.g., 0.1 mm (Martin-Vide and Gomez 1999; Brunetti et al. 2002)—or by dry spells, where a dry spell is defined as a period in which the daily precipitation amounts do not exceed a given threshold. Vicente-Serrano and Begueria (2003) give an excellent summary of the methods, including the list of possible thresholds. Fifteen consecutive days with rainfall less than 0.25 mm, or 0.1 mm, are required (Heim 2002) to indicate a drought in Britain.

Vicente-Serrano and Begueria (2003) point out that drought indices are not as useful in identifying spatial patterns of drought risk since they are based on standardized or normalized shortages in relation to "average conditions," which relate to a given station and a given period. This holds true for both the SPI and the PDSI indices. As a result, the frequency of drought spells is about the same for all stations no matter if they lie in extremely arid or extremely rainy regions, even though the rainy sites may receive several times more rain than the arid sites. Similarly, these indices cannot be used in climate-change impact assessments, as they would provide approximately the same distributions for both present and changed climates regardless of the changes in the climatic conditions. To allow for comparisons of drought conditions in different locations, Vicente-Serrano and Begueria (2003) prefer to define dry spells as a continuous period with daily precipitation less than or equal to 0.1 mm or 5 mm. They also provide many references to studies made by other authors who used a similar approach but having different thresholds.

The main aim of this paper is to introduce the relative SPI and PDSI indices, and to use them for assessing possible impacts of the forthcoming climate change on drought characteristics in Czechia. The new versions of both indices are called the "relative drought indices." They can be used for between-station comparisons, making them potentially useful in any spatial analysis of drought conditions. The relative indices are first calculated using monthly weather series from 45 Czech stations to assess present climate drought conditions. To assess future climate drought conditions, the drought indices are then derived from weather series obtained by modification of the observed series according to five GCM-based climate-change scenarios.

2. Data

2.1. Station weather data

The climate of Czechia is generally temperate. According to the Kőppen classification (Oliver 2005, p. 218), the majority of its territory is classified as *Cfb*, which changes to *Dfb* and *Dfc* with increasing altitude (Tolasz et al. 2006). The *Cfb* climate implies at least 30 mm of precipitation each month, with the warmest month's average temperature being below 22°C but having at least 4 months with an average temperature above 10°C; *Dfb* and *Dfc* differ from *Cfb* by having lower temperatures. The continentality of the climate increases from west to east, which is reflected in the increasing amplitude of the annual temperature cycle in a zonal direction (0.13 ± 0.04 K per longitude degree). The driest climates are found in the Central Bohemian basin and in the southeast, the latter region also being the warmest in Czechia. However, the spatial variability of the climate is mostly due to orography, with the largest degree of variability of most climate characteristics being related to altitude.

The present analysis is based on 40 years (1961–2000) of observational data from 45 Czech stations; the station locations are displayed in figure 1 and their basic characteristics are given in table 1. The set of stations represents the longitudinal-latitudinal-altitudinal extent of the Czech territory well. Figure 2 shows that the annual mean temperature nearly linearly decreases from 9.5 to 3.3°C as the altitude of the stations increases from 158 to 1,324 m a.s.l. [in reality, the altitude of Czechia ranges from 115 m (the location where the Labe River leaves the Czech territory) to 1,602 m a.s.l. (Snezka Mountain)]. The mean annual precipitation exhibits positive correlation with the altitude and ranges from 449 to 1,406 mm.

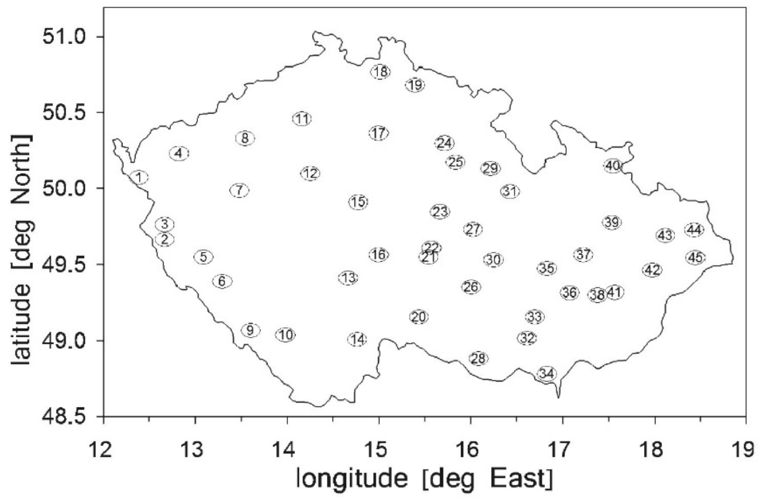

Figure 1. Czechia and location of the 45 stations used in the analysis. See table 1 for the list of the stations.

Table 1. List of stations (arranged from west to east)

Station			Long	Lat	Alt	TAVG	PREC	SWHC
Idx	Abbreviation	Name	(deg)	(deg)	(m a.s.l.)	(deg C)	(mm)	(mm)
1	CHEB	Cheb	12.390	50.074	471	7.7	566	223
2	PRIM	Primda	12.680	49.669	742	6.4	698	165
3	PERN	Pernolec	12.680	49.767	530	7.5	610	213
4	KRAU	Krasne Udoli	12.830	50.233	647	6.4	606	158
5	STAN	Stankov	13.100	49.550	370	8.2	537	158
6	KLAT	Klatovy	13.300	49.392	430	8.3	595	158
7	KRAL	Kralovice	13.490	49.989	468	7.8	486	165
8	ZATC	Zatec	13.550	50.333	201	9.2	449	158
9	CHUR	Churanov	13.610	49.068	1,118	4.9	1,085	213
10	HUSI	Husinec	13.990	49.040	536	7.7	639	165
11	DOKS	Doksany	14.170	50.459	158	8.8	449	218
12	RUZZ	Praha–Ruzyne	14.260	50.101	374	8.2	511	237
13	TABO	Tabor	14.670	49.414	437	8.0	570	158
14	TREB	Trebic	14.770	49.009	429	7.8	614	22
15	ONDR	Ondrejov	14.780	49.911	526	7.9	665	165
16	LUKA	Lukavec	15.000	49.567	610	7.7	636	165
17	SEMC	Semcice	15.000	50.367	234	9.0	581	140
18	LIBC	Liberec	15.020	50.769	398	7.6	818	213
19	VYSO	Vysoka nad Jizerou	15.400	50.683	670	6.7	1,015	213
20	KMYS	Kostelni Myslova	15.440	49.160	569	7.4	588	165
21	HUMP	Humpolec	15.550	49.550	525	7.1	665	165
22	HAVL	Havlickuv Brod	15.580	49.612	455	7.6	672	213
23	CASL	Caslav	15.670	49.850	263	8.8	522	213

24	HNEV	Hnevceves	15.720	50.300	265	8.8	617	237
25	HRAD	Hradec Kralove	15.840	50.176	278	8.8	617	158
26	VMEZ	Velke Mezirici	16.010	49.354	452	7.4	584	165
27	SVRA	Svratouch	16.030	49.735	737	6.3	767	192
28	KUCH	Kucharovice	16.090	48.883	334	8.8	475	260
29	KOST	Kostelec	16.220	50.133	290	8.2	690	237
30	DOMA	Domaninek	16.250	49.533	560	6.8	592	165
31	USTI	Usti nad Orlici	16.430	49.983	557	7.6	760	165
32	ZABC	Zabcice	16.620	49.017	179	9.4	471	218
33	BTUR	Brno–Turany	16.700	49.160	241	9.1	489	260
34	LEDN	Lednice	16.830	48.783	171	9.5	486	218
35	PROT	Protivanov	16.830	49.477	670	6.6	650	192
36	IVAN	Ivanovice	17.080	49.317	225	8.7	555	260
37	OLOM	Olomouc–Slavonin	17.230	49.567	225	8.8	555	218
38	KROM	Kromeriz	17.380	49.300	204	9.1	570	260
39	CERV	Cervena	17.540	49.778	750	5.9	745	192
40	ZARY	Zary	17.550	50.152	483	7.7	752	165
41	HOLE	Holesov	17.570	49.319	224	8.8	625	260
42	VALM	Valasske Mezirici	17.980	49.464	334	8.3	767	158
43	MOSN	Mosnov	18.120	49.694	251	8.5	701	218
44	LUCI	Lucina	18.440	49.731	300	8.3	833	158
45	LYSA	Lysa hora	18.450	49.546	1,324	3.3	1,406	212

TAVG mean annual temperature, *PREC* mean annual precipitation, *SWHC* soil water-holding capacity

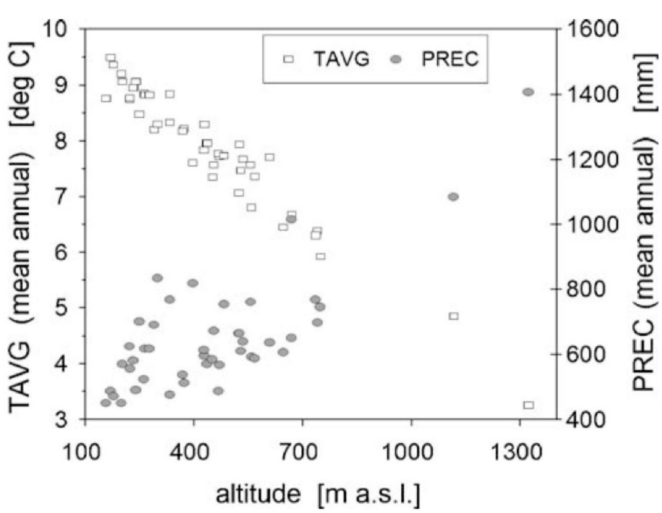

Figure 2. The mean annual temperature and precipitation vs. altitude for the 45 Czech stations.

2.2. GCM-based climate-change scenarios

To assess the impact of climate change on drought conditions in Czechia, we used outputs from the GCM simulations, which were utilized in the IPCC's Third Assessment Report (Houghton et al. 2001). The model outputs were downloaded from the IPCC Data Distribution Center (http://cera-www.dkrz.de/IPCC_DDC/SRES/index. html). Of the available GCM outputs, we employed (i) only simulations made using the SRES-A2 emission scenario, which assumes the highest CO_2 emissions when compared to the other SRES scenarios, and (ii) only five GCMs, whose output series include the 1961–2099 period: CSIRO-Mk2, CGCM2, GFDL-R30, HadCM3, CCSR/NIES. All GCMs included in the analysis are coupled models incorporating ocean circulation. The horizontal resolution for the atmospheric part of the model ranges from 2.8 to 7.5° in the zonal direction and from 2.25 to 5.6° in the meridional direction. The details of the models may be found on the IPCC's web page, given above.

The climate-change scenarios were derived from the GCM-simulated monthly time series as a difference (for temperature) or ratio (for precipitation) between the monthly means of the end-of-21st-century series (2060–2099) and end-of-20th-century series (1961–2000). The scenarios were interpolated (from the surrounding grid boxes) to a location defined by latitude = 49.5°N and longitude = 16°E, which is close to the center of Czechia. Since the variability of the climate-change scenarios over the Czech territory is much smaller compared to the inter-GCM variability (Dubrovsky et al. 2005), we used the same set of climate-change scenarios for all stations. To obtain a monthly series that would represent the changed climate for a given station (and would be used as input into the SPI and PDSI indices), the scenario increments displayed in figure 3 were added to the individual observational station series.

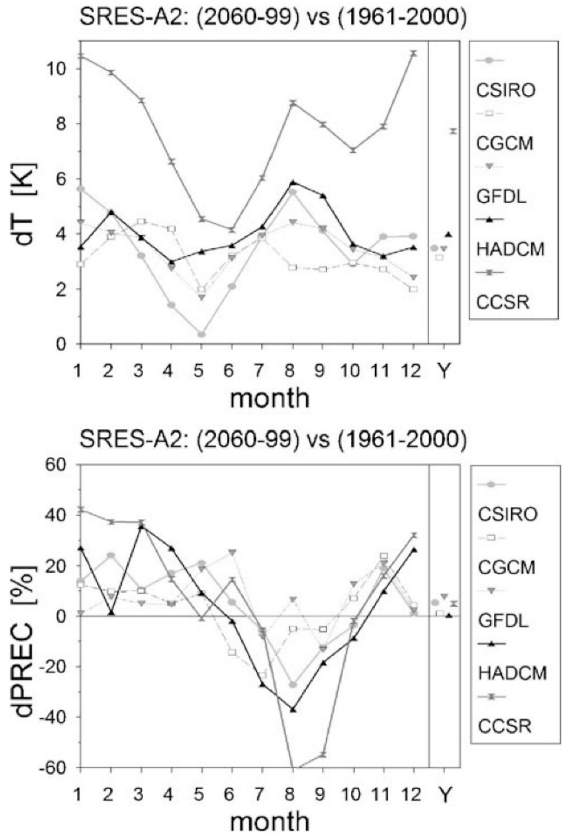

Figure 3. Climate-change scenarios based on five GCMs (A = CSIROMk2, C = CGCM2, G = GFDL-R30, H = HadCM3, J = CCSR/NIES AGCM + CCSR OGCM). The GCMs were run using the SRES-A2 emission scenario, and the climate-change scenarios are interpolated for a location defined by latitude = 49.5°N and longitude = 16°E, which is close to the center of Czechia.

3 Methods

The SPI

The Standardized Precipitation Index (SPI) is the transformation of a given precipitation amount aggregated over a selected period (commonly 1 to 24 months, where the shorter time scales may represent agricultural drought and the longer time scales relate better to hydrological drought) into a standardized normal distribution (http:// drought.mssl.ucl.ac .uk/spi.html). A gamma distribution is commonly used to approximate the observed probability distribution function of the precipitation amount. Methods of estimating the parameters of the distribution were reviewed by Lloyd-Hughes and Saunders (2002) and the effect of the length of the precipitation record on the SPI was analyzed by Wu et al. (2005) and Guttman (1994). Other distributions may also be used. For example, the Poisson-gamma distribution was used by Lana et al. (2001), a log-normal distribution was discussed by Lloyd-Hughes and Saunders (2002), and Guttman (1999) used an L-moment analysis and found the Pearson III distribution to be the best, followed by the gamma distribution. The present version of SPI uses a gamma distribution whose parameters are estimated separately for each of the 12 months of the year. Having the gamma distribution parameters estimated from the input precipitation series, precipitation amounts (*PREC*) are transformed into probabilities and then run through the SPI: SPI = F^{-1}[G(PREC)]; where G is the cumulative gamma distribution and F^{-1} is the inverse standard normal distribution. Because of common problems in fitting the tails of the distributions, the SPI values which fall outside the (−2, +2) range should be used with care. Five temporal aggregations are used here: 1 month, 3 months, 6 months, 12 months, and 24 months; the corresponding indices are denoted as SPI-1, SPI-3, SPI-6, SPI-12, and SPI-24.

The PDSI

Palmer published his method for calculating the PDSI in 1965 (Palmer 1965). Unlike the SPI, the PDSI is based on more than just precipitation. The PDSI actually uses a supply and demand model for the amount of moisture in the soil. The value of the PDSI is reflective of how the soil moisture compares with normal conditions. A given PDSI value is calculated by using a combination of the current conditions along with previous PDSI values, so the PDSI also reflects the progression of trends to determine whether it is in a dry or a wet spell. That means that a single PDSI value is not representative of just the current conditions but also of recent and antecedent conditions to a lesser extent. The algorithm used here for calculating the PDSI is described at http://nadss.unl.edu/PDSIReport/pdsi/self-cal.html. This version coincides with the self-calibrated PDSI, in which the following parameters of the PDSI model are derived from the input weather series: (1) duration factors; (2) climatic characteristics (parameter K′, and 2% and 98% percentiles of the "first-round" PDSI); (3) water balance coefficients (α, β, γ, δ); and (4) the Thornthwaite heat index and Thornthwaite exponent used in calculating the evapotranspiration. Station-specific soil water-holding capacities were determined from the soil map of Czechia (Tomasek 2000).

Self-calibrated vs. relative indices

It follows from the above discussion that the process of calculating both SPI and PDSI series consists of two steps: in the first step, parameters of the model are calculated; in the second step, the values of the drought index are determined. In the case of the self-calibrated SPI and PDSI, the same weather series (precipitation series for SPI; precipitation plus temperature series for PDSI) is used in both steps. This relates to the fact that these indices are designed to express drought severity with respect to normal conditions at a given site. The result of the self-calibration process is that the range of either drought index is about the same for each station and/or period represented by the input weather series (SPI is within < –2, +2 > with about 95% probability, and PDSI is within < −4, +4 > with about 96% probability), and therefore these indices cannot be used for between-station comparisons of absolute drought conditions, nor for between-period (essential in assessing the potential impacts of climate change) comparisons. For example, a SPI of +2 for a station in an arid area represents completely different drought conditions than the same value for a station in precipitation-rich area. Being inspired by Wells et al. (2004), we shall call these indices (both SPI and PDSI) the *self-calibrated indices*.

In our paper, we introduce the relative indices, which can be used either to compare drought conditions at different sites during a given period or to compare drought conditions for a single site during different periods. The relative indices differ from the self-calibrated indices by using two different weather series in the two-step process. In the first step, the model of the drought index is calibrated using the reference weather series, which may either relate to some reference station (in between-station comparisons), or to a reference period (in between-period comparisons). Having calibrated the model, it is then applied to the second series, hereafter called the tested series. The tested series relates either to the different station (to compare the drought conditions in that station with respect to the reference station) and/or to the different period (to compare drought conditions in that period with respect to the reference period). Alternatively, we use the reference series created by aggregating data from a set of stations in our analysis. In this case, the resultant reference series represents a wider spectrum of precipitation-temperature situations, which should make the model applicable for a wider spectrum of climatic conditions. From now on, we shall denote the two relative drought indices as rSPI and rPDSI, while scSPI and scPDSI will be used for the self-calibrated indices. SPI and PDSI symbols will be used when both types of the indices are under question or when we discuss the properties that are common for both the self-calibrated and relative indices.

The executable models for the relative indices were obtained by modifying the original self-calibrated indices available from the University of Nebraska–Lincoln (Computer Science and Engineering, and National Drought Mitigation Center). The original version of the PDSI is described in Wells et al. (2004).

Drought spells may be identified from the time series of the drought index values. In the present analysis, the SPI-based drought spell is defined as a continuous period in which the SPI is always below 0 and its minimum value falls below −1. The PDSI-based spell is the period in which the PDSI is always below –1 and its minimum value falls below –3. The definition for drought spells was inspired by Huth et al. (2001), who defined heat and cold waves using two temperature thresholds. We should note, however, that other authors often use a single-threshold definition for drought spells, whether using the SPI or PDSI (Lloyd-Hughes and Saunders 2002; Zou et al. 2005). Having defined the respective drought spells, we might derive their various characteristics (e.g., duration and intensity), but for our purposes we shall study only one characteristic here: the number of months which are included in a drought spell.

Figure 4 demonstrates the temporal structure of the time series of drought indices derived from the present climate precipitation data. Note how the intermonthly variability of scSPI decreases as the time aggregation increases. Of all time aggregations of scSPI studied here, the correlation with scPDSI (correlation coefficients are displayed in fig. 4) reaches its maximum for the 12-month scSPI. This corresponds to the results obtained by other authors already cited in the introduction (Lloyd-Hughes and Saunders 2002; Redmond 2002; Bordi and Sutera 2001). In general, the trends in individual SPI indices are statistically insignificant (not shown here), which relates to the insignificant trend in annual precipitation (−1 ± 11 mm per 10 years for the annual precipitation sum averaged over the 45 stations, −3 ± 15 mm per 10 years for the Svratouch station shown in fig. 4). In contrast, the PDSI trends exhibit a statistically significant negative trend (−0.54 ± 0.07 per 10 years), indicating increased drought risk, which is related to the increasing temperature trend (0.3 ± 0.1 K per 10 years for the annual temperature averaged over the 45 stations as well as for the Svratouch station). These results (trends and correlations between indices) are very similar for the other stations used in our analysis.

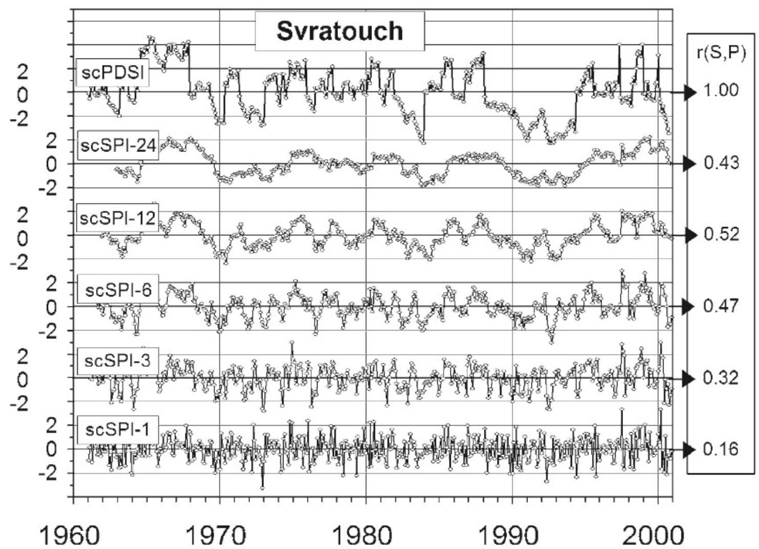

Figure 4. Time series of the self-calibrated drought indices derived from the Svratouch station weather series. The *numbers* in the box on the right side of the graph are the correlation coefficients of the given series with the PDSI.

4. Results

4.1 Relative vs. self-calibrated indices

Figure 5 displays the relationship between the scSPI and rSPI. The latter was calibrated using either weather series from a single reference station (empty circles marked as "wrt Hradec") or data aggregated from all stations (rectangles marked as "wrt ALL"); examples of a 1- and 12-month rSPI for the Lysa hora station are shown. In both calibration approaches the relationship is near-linear for each single calendar month, but the regression lines (not shown in the figure) differ somewhat for individual months (especially in the "wrt Hradec" series, whose values for June and November are marked by symbols in the figure). The latter situation is explained by the fact that the SPIs are calibrated separately for each month. Note that the values of rSPI are higher than those of scSPI, which indicates that the precipitation sums in the tested station (Lysa hora) are larger than those of the reference station. Because of the computational problems with approximating the extreme values with the gamma distribution, the values of the SPI had to be limited within some finite bounds. These bounds were selected (subjectively by the programmer) to be −5.55 and +5.55 (the upper bound values occur in the "wrt Hradec" series shown in fig. 5); this implies that the normally distributed value would fall outside this interval with 3×10^{-6}%

probability. The fitted distribution does not clearly provide an accurate approximation of the distribution function tails, thus the values close to the upper or lower limits merely indicate that the precipitation is very small or very large. Occurrence of the beyond-limits values in the relative index series indicates that the precipitation sums are far above (or below) the values found in the reference station series. As was expected, when calibrated with all-station data, the rSPI values do not exceed these limits. The nearly perfect linear relationship between the self-calibrated and relative SPIs implies that the time series of three versions of the SPI (self-calibrated, calibrated with single station, and calibrated with an aggregate of several weather stations) are in parallel (see the top and middle panels in fig. 6) and exhibit the same temporal structure. In fact, they differ only in their bias and the scale factors, except for the middle series in the middle panel. In this case, the rSPI values often reach the upper limit and then remain unchanged for many consecutive months, thereby providing no information on the evolution of the dry/wet conditions. However, except for this limitation, all three versions of the SPI provide similar information applicable for monitoring the evolution of droughts.

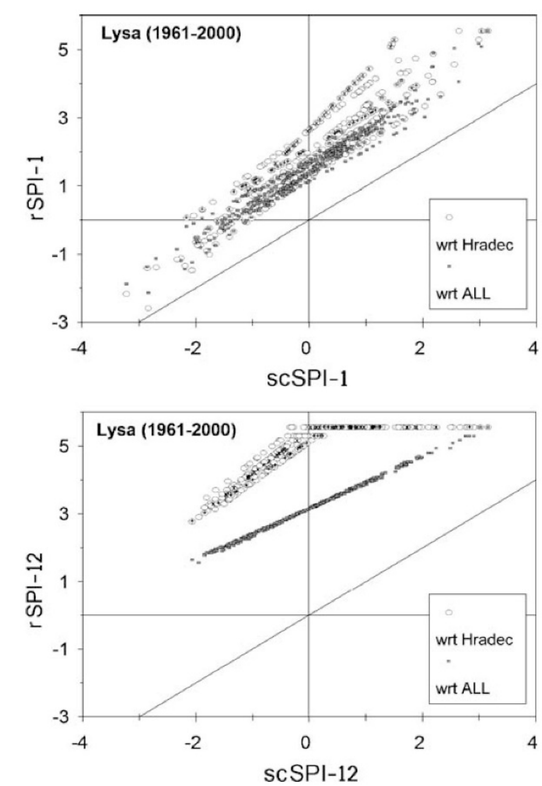

Figure 5. The relationship between the self-calibrated and relative SPI for Lysa hora station. The SPI is calibrated using station data from Hradec Kralove ("wrt Hradec" series; circles marked with symbols x and + relate to November and June) and an aggregate of data from all stations ("wrt ALL" series).

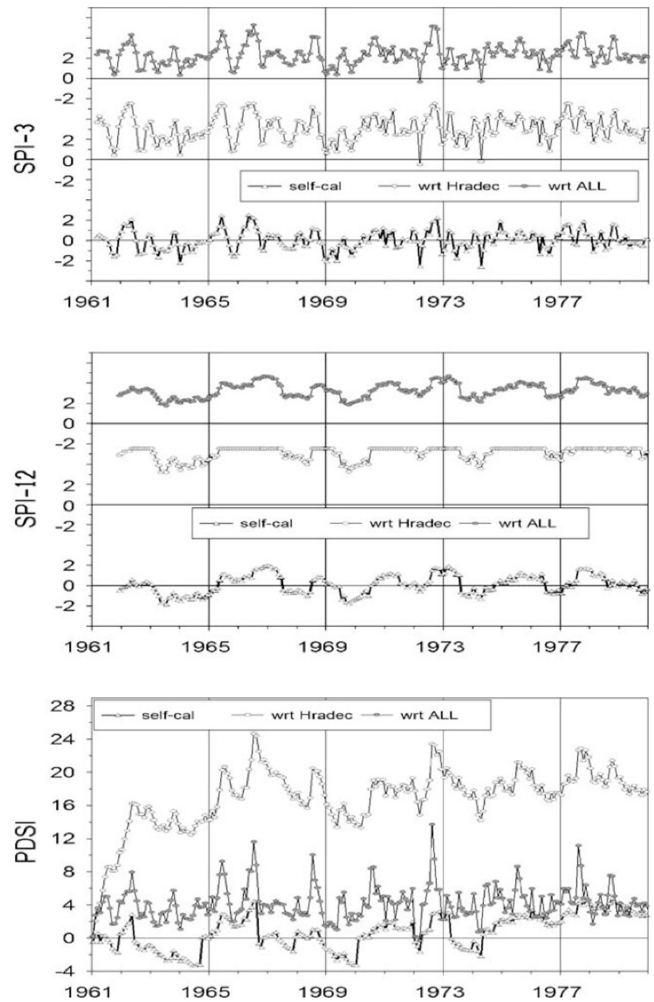

Figure 6. Time series of the self-calibrated ("self-cal") and relative (single-station calibrated = "wrt Hradec," all-station-calibrated = "wrt ALL") SPI-3, SPI-12, and PDSI for the Lysa hora station.

The corresponding graphs for the PDSI look much more complicated. The correlation between the self-calibrated and relative PDSI is not as close (fig. 7), and consequently the time series of scPDSI and rPDSI (note the bottom panel in fig. 6) do not align as nicely when compared to the SPI. Fortunately, the information on the relative changes (decreasing or increasing trends) is generally present in the time series of the rPDSI calibrated using a single-station weather data approach. In the case of the rPDSI calibrated utilizing all-station data, the time series is very noisy and therefore the information on the intermonthly changes in drought conditions and short-term trends provided by such rPDSI does not satisfactorily correlate with the information provided by the scPDSI. However, the mean climatological (e.g., 40 years used here) value of this rPDSI might be used to assess mean drought-climatology conditions. We have found only small differences in drought trends derived using single-station and all-station-calibrated rPDSI values. Two features are worth noting:

1) The relationship between the self-calibrated and relative PDSI shown in figure 7 exhibits a vivid "discontinuity" when scPDSI values are around zero. The discontinuity is related to the presence of sudden drops or increases toward close-to-zero values in the scPDSI series (also found in fig. 6). These abrupt changes are due to the "backtracking" procedure involved in the underlying PDSI model. This procedure accounts for the probability of the current spell ending by switching between three intermediate PDSI values. Seemingly, if the tested station is too wet or too dry with respect to the reference station, the model takes the whole series to be either a single wet or dry spell and no switching is applied.

2) Both scPDSI and rPDSI series always starts with a zero value and it takes several months before the index reaches a meaningful value. This spin-up time in the rPDSI series increases with increasing differences between the tested and reference series. For example, 6–8 months are needed in figure 6 before the rPDSI (calibrated with a single reference station) starts to run parallel with the scPDSI.

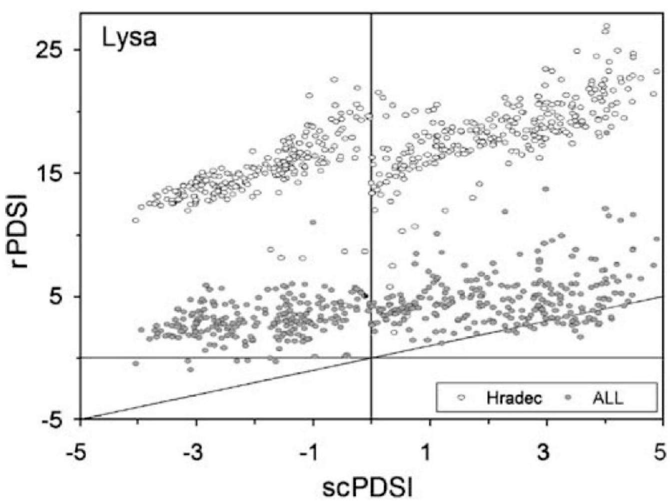

Figure 7. Relative vs. self-calibrated PDSI for the Lysa hora station. rPDSI is calibrated using single-station data ("Hradec") and all-station data ("ALL").

4.2 Impact of climate change

The present climate drought conditions for the 45 stations are shown in figure 8 in terms of the relative indices. The indices were calibrated using an aggregate of all station data, and then applied separately to each single station. For the rSPI, this figure shows that the sensitivity of the index increases as the time-aggregation period increases. This increasing sensitivity is manifested by a decreasing number of stations having a drought month frequency higher than zero and lower than 100%. In the case of rSPI-24, five stations exhibit

100% frequency of drought months and 15 stations encounter no drought months, which may seemingly lessen the applicability of such drought spell definitions for these stations. The sensitivity of the index is related to the ratio of variability of a single-station rSPI to the between-station variability of rSPI means. As the variability of the precipitation sum decreases with increasing time aggregation, this ratio also decreases, which implies that the time series for an increasing number of stations are classified to be either in a single drought spell or a single nondrought spell. In this context, the rPDSI exhibits the greatest sensitivity of all indices, which is probably due to its dependence on both temperature and precipitation. Figure 2 shows that the drier (wetter) stations mostly encounter warmer (colder) temperatures. As a result, inclusion of the temperature generally amplifies drought conditions in low precipitation stations and exaggerates wet conditions in the higher precipitation stations. This makes the spectrum of rPDSI-based drought conditions wider (compared to rSPI), and consequently a larger number of stations tend to be either always dry or always wet (see fig. 8). One may also note that the percentage of drought months is nearly the same in all four seasons, which is due to calibration being made separately for each month of the year.

In assessing the impact of forthcoming climate change on drought conditions for these 45 stations, the characteristics of the drought indices derived from the future-climate monthly weather series (obtained by the direct modification of the present observed series) are compared with those derived from the station observational monthly weather series.

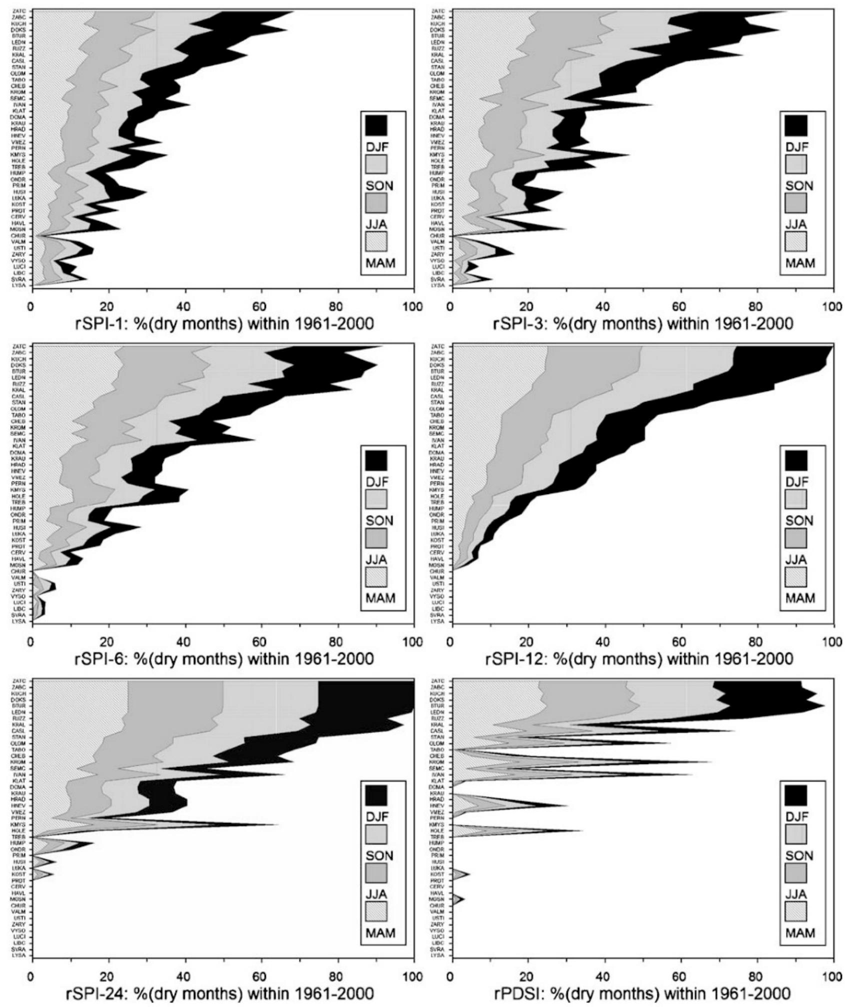

Figure 8. rSPI-1, rSPI-3, rSPI-6, rSPI-12, rSPI-24, and rPDSI for the present climate based on 45 stations in Czechia: percentage of months within dry spells during 1961–2000; reference station = aggregate of all 45 stations. (Stations are arranged according to the frequency of dry months in SPI-12-based drought spells).

Since the SPI is based only on precipitation, the changes in rSPI-1 and rSPI-12 (figs. 9 and 10) closely follow the precipitation changes prescribed by the climate-change scenarios shown in figure 3. For example, a projected increase in winter precipitation implies an increase in rSPI-1 (top-left panel in fig. 9) with a decreasing frequency of rSPI-based dry months (top-right panel in fig. 9). Conversely, a decrease in summer precipitation implies a decrease in rSPI-1 (middle-left panel) with an increasing frequency of rSPI-based dry months (middle-right panel). For a whole year, slight changes in the annual precipitation sum imply slight changes in the annual rSPI characteristics (bottom panels). Figure 10 shows that the rSPI-12 is less affected by climate change when compared to rSPI-1 (fig. 9). This relates to the fact that the rSPI-12 transforms 12 months of precipitation; therefore its mean annual cycle is diminished and the changes in any month or season of the year are nearly the same and very slight since they are closely correlated with the annual precipitation, which is projected to exhibit only subtle changes.

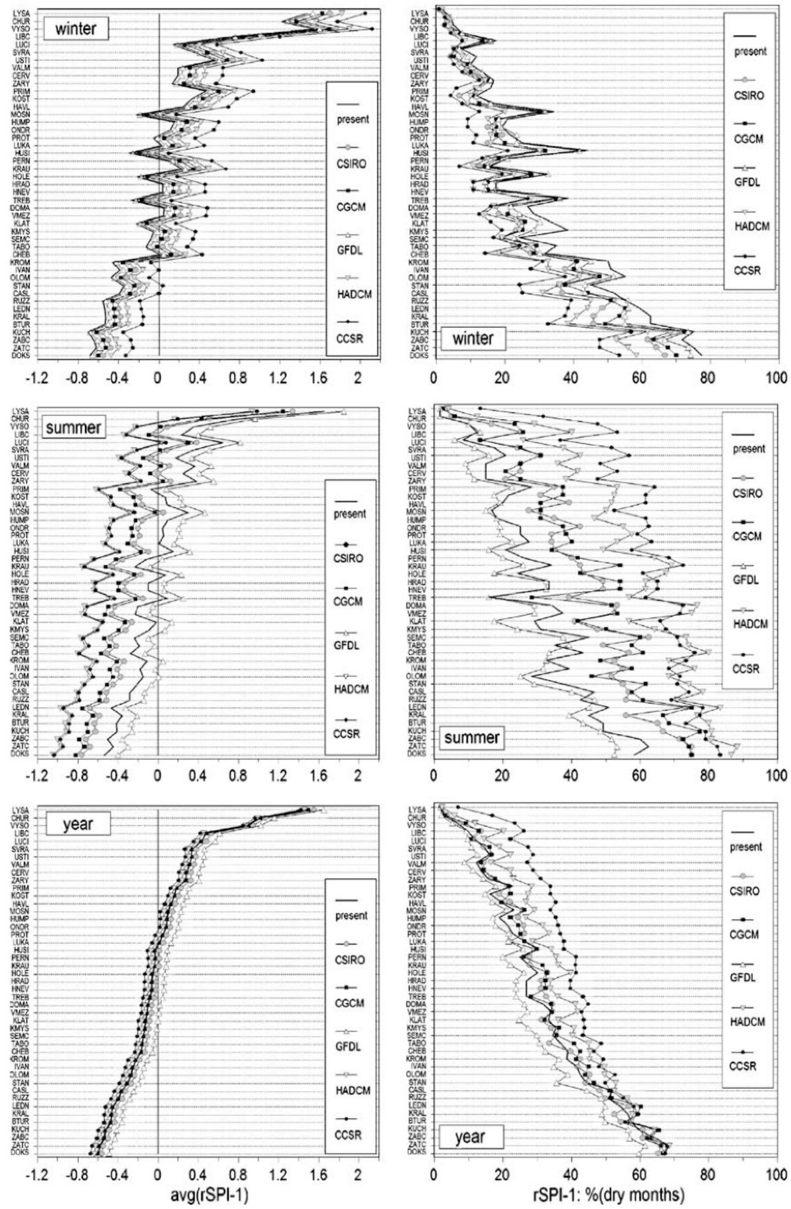

Figure 9. Relative (calibrated with all-station data) SPI-1 in the present and changed climates. Left: average value of relative SPI in winter/summer/annually. Right: percentage of SPI-1-based dry months in summer/winter/annually (stations are arranged according to the average value of rSPI-1).

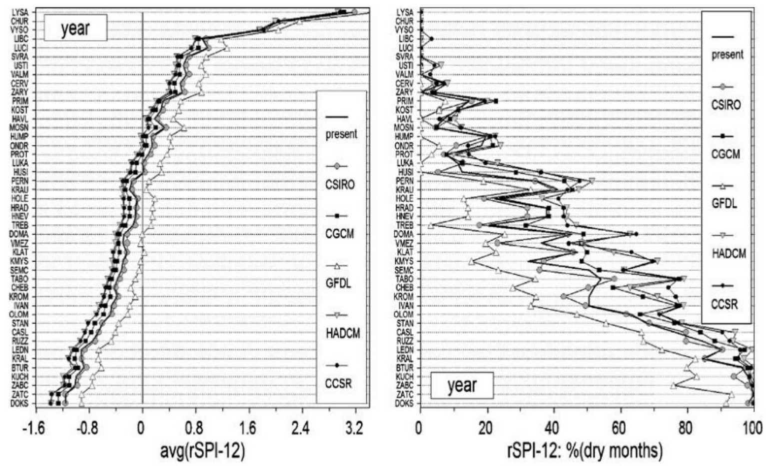

Figure 10. Same as figure 9, but for the SPI-12 and the whole year.

In contrast to the rSPI, the changes in the rPDSI are due to changes in both precipitation and temperature. Figure 11 shows that the drought risk indicated by the mean value of rPDSI will significantly increase in both winter and summer under each of the five GCM-based scenarios. In summer, the increase in drought risk due to decreased precipitation will be augmented by increasing temperature. In winter, the effects of the temperature rise and decreasing precipitation will act in opposite directions, but the effect of increased temperatures will dominate. Because of the persistence of the drought index (note in fig. 4 that some dry or wet periods can last for several years) with no apparent annual cycle being involved, the difference between the summer and winter changes is small. The most significant effect of climate change on the rPDSI values is found in the CCSR/NIES scenario, which exhibits the most significant temperature rise (fig. 3).

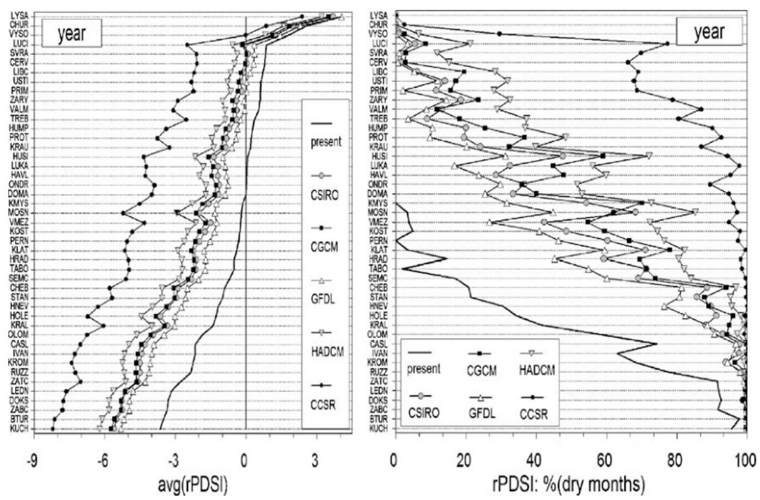

Figure 11. Relative (calibrated with all-station data) PDSI in the present and changed climate. Left: average value of rPDSI in a whole year. Right: percentage of rPDSI-based drought months in the 40-year series.

Figures 9–11 may be used to make assumptions about the shifts of the Czech stations' drought conditions due to climate change. For example, in summer under the CCSR/NIES scenario, nearly 70% of stations may encounter drier (in terms of mean rPDSI values) conditions compared to the driest station under the present climate (fig. 11). This shift is, however, lower in other GCMs (because of lower temperature increases) as well as in the case of the rSPI index, which is affected only by precipitation changes. In summer, the shift in rSPI-1 is large but the shift in winter is found to be in the opposite direction (toward wetter conditions) so that the shift in the annual mean of rSPI-1 (as well as of rSPI-12) is very small. Our results may suggest that the growing season will be negatively affected by more frequent summer droughts.

Another approach to assessing the effect of the predicted climate change on drought risk is depicted in figure 12. In contrast to previous experiments, where the indices for each station were calibrated with observational data aggregated from all stations, the drought indices are now calibrated using a given station's data and then applied to the future-climate weather series obtained by modification of the observational data according to the climate-change scenario. Thus, figure 12 displays the future-climate drought conditions in terms of rSPI-1 and rPDSI, both being calibrated with the present-climate weather series. The left panels show the average values of the two indices and the right panels show how the number of drought months will increase under the climate-change scenario. While the average values of the self-calibrated indices are close to zero (the between-station differences in the average values of the two drought indices are not considered to be significantly different from zero) as a consequence of the self-calibrating procedure, the average values of the future-climate drought indices show that: (a) rPDSI values will be much lower (under all climate-change scenarios), resulting in a large increase in drought month occurrences with the percentage of months falling within drought spells approaching 100%; (b) the average rSPI-1 values will rise in winter by 0.04 (under the GFDL scenario) to 0.6 (CCSR/NIES scenario) as a consequence of the precipitation increase during this season, resulting in a decrease of drought month occurrences by a few months in the GFDL scenario up to approximately 50% in the CCSR/NIES scenario; and (c) in summer, the rSPI-1 will decrease in all but the GFDL-based scenario as a consequence of the precipitation decrease. The decrease of rSPI values will result in an increase of drought month frequency, which will more than double under the HadCM3 and CCSR/NIES scenarios. Overall, the message in figure 12 is similar to those of previous figures related to the rSPI-1 (fig. 9) and rPDSI (fig. 11). However, while the latter figures allow for between-station comparisons of drought conditions, figure 12 shows how the values of drought indices will change in the future in terms of the present-climate conditions.

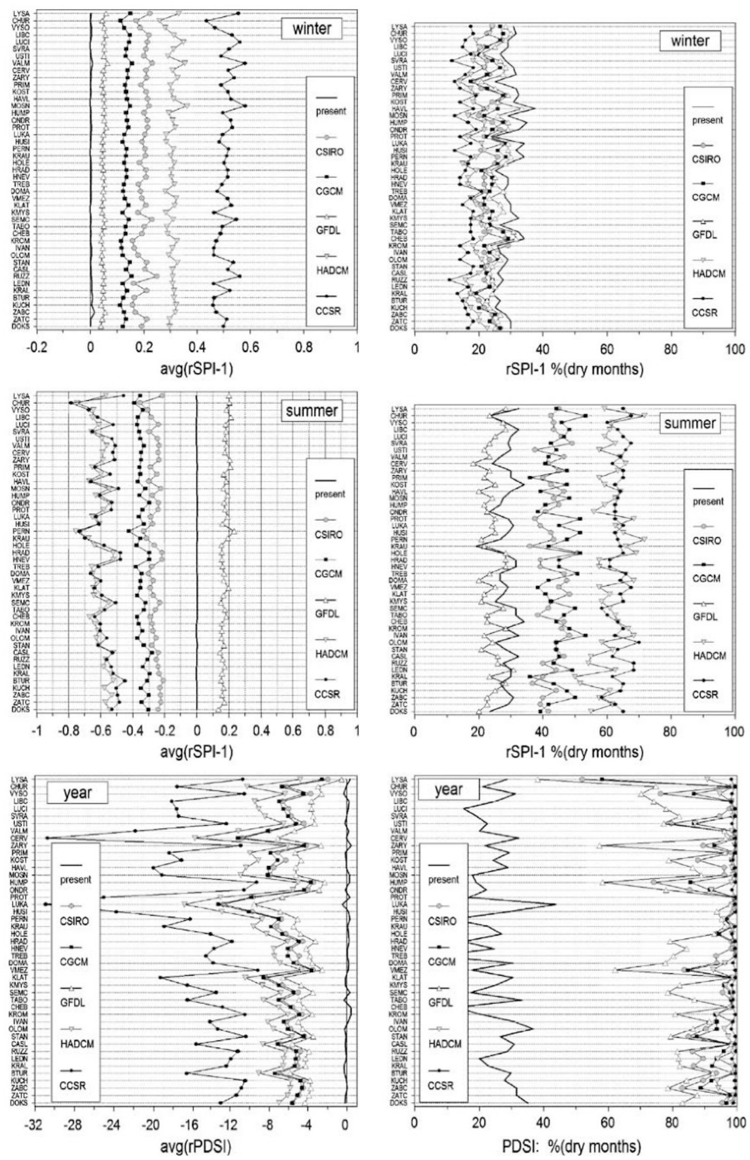

Figure 12. Left: average value of the rSPI-1 (top: winter; middle: summer) and annual rPDSI (bottom) for the changed climate; the indices were calibrated with the weather series observed at the given station. Right: percentage of months within the drought spells.

5. Conclusions

PDSI and SPI drought indices were used in the present paper to assess drought conditions in Czechia under both present and future climates. Of the five time aggregations of SPI (ranging from 1 month to 24 months), the 12-month SPI exhibits the closest correlation with the PDSI. Since the self-calibrated drought indices (both scSPI and scPDSI) cannot be used in assessing climate change, the relative drought indices, rSPI and rPDSI, were defined and utilized in this paper. These indices are calibrated using the reference series as a first step and are then applied to the other weather series. As a result, the relative indices allow for the comparison of drought conditions in the latter series with respect to the reference series. This feature may be used to compare drought conditions at different locations or to compare drought conditions at one site, but for different periods. In our experiments, the drought indices were calibrated by using precipitation and temperature data either from a single reference station, or aggregated from all stations. Comparisons between the relative and self-calibrated drought index series shows that:

i. The rSPI is highly correlated with the scSPI. In fact, the time series of the two types of SPI are in parallel to one another so that except for the absolute value, the information provided by them is the same. Specifically, both indices give the same information on trends or intermonthly variability in drought conditions.

ii. The rPDSI calibrated with a single station is also closely correlated with scPDSI, but the correlation is not as close as in the case of SPI and therefore some drought characteristics (e.g., duration of the drought spell) may differ. The calibration using all-station weather data deteriorates the information provided by the rPDSI even more significantly; the temporal structure of the resultant rPDSI significantly differs from the structure of the scPDSI series. This implies that drought spells estimated from the rPDSI calibrated in this way would be quite different from those identified in the scPDSI series (even after correcting the rPDSI series for the systematic bias).

The relative indices were then used to compare the present climate drought conditions at 45 Czech sites (fig. 8) and to assess the potential impact of forthcoming climate change on droughts and their characteristics in Czechia. The former experiment shows that:

iii. For the rSPI, the sensitivity, which is related to the ratio of variability of a single-station SPI to the between-station variability of SPI means, increases as the time-aggregation period increases. The increasing sensitivity is manifested by an increasing number of stations having a drought month frequency of either zero or 100%.

iv. Of all drought indices studied here, the rPDSI values are the most sensitive to the mean climatic conditions at a given station. This is explained by the dependence of rPDSI on both precipitation and temperature, which are strongly negatively correlated, thereby widening the spectrum of drought-specific climatic conditions over all stations. As a result, the whole weather series in a larger number of stations may be classified as totally dry (all months fall into drought spells) or totally wet (no drought spell occurs) when using the rPDSI. This, however, does not imply a problem for the between-station or between-period comparative studies.

The results of the climate-change impact analysis indicate:

v. Changes in the rSPI values closely follow changes in precipitation (which is not surprising given that the SPI is based on a transformation of a precipitation sum accumulated over a given period). As the precipitation is predicted to decrease in summer and increase in both winter and spring, drought risk tends to increase (decrease) in the respective season. Since the rSPI-1 is not affected by persistence, the seasonality in drought changes indicated by the rSPI-1 directly follows the seasonality of the precipitation changes. On the other hand, drought changes indicated by the rSPI-12 follow the projected annual precipitation changes, which are only minimal.

vi. Changes in the rPDSI, which is influenced by both precipitation and temperature (temperatures are predicted to increase under all climate-change scenarios), indicate an increased drought risk for all stations under all climate-change scenarios. Because of the dependence of drought on temperature, we think that the rPDSI is more appropriate (when compared to the rSPI) for use in assessing the potential impact of climate change on future droughts.

vii. Two approaches to assessing the impact of climate change on drought conditions were employed. In the first approach, the drought indices were calibrated using an aggregate of observational (1961–2000) data from all stations and were then applied to both the present-climate and future-climate weather series for each individual station. In the second approach, the drought indices were calibrated using observational data from a given station and then applied to the future-climate weather series obtained by modification of that station data according to the climate-change scenario. While the former approach allows for between-station comparisons of drought conditions and assessment of their spatial shifts due to climate change, the latter approach allows the user to assess how the values of drought indices will change in the future with respect to the local present-climate conditions (which local users may find more useful, compared to the former approach).

The present climate-change impact analysis was performed for five GCM-based climate-change scenarios, which were related to the end of 21st century. These GCMs were run applying a single emission scenario—SRES-A2, which is considered to be the most pessimistic amongst the four marker SRES emission scenarios, as this particular emission scenario assumes the highest CO_2 increases. Therefore, changes in drought conditions may be correspondingly lower for less pessimistic emission scenarios or for less distant future.

Acknowledgments – The present study was sponsored by the Grant Agency of the Czech Republic (Project 205/05/2265—"Calibration of Weather Generator for Sites without or with Incomplete Meteorological Observations") and by the Ministry of Education, Youth and Sports of the Czech Republic (Research plan No. MSM6215648905, "Biological and Technological Aspects of Sustainability of Controlled Ecosystems and their Adaptability to Climate Change"). We also acknowledge support from the KONTAKT project ME 844, which has enabled intensive cooperation between the authors. We are grateful to Shifeng Zhang (Computer Science & Engineering Department, University of Nebraska–Lincoln), who made the necessary modifications to the source code of the PDSI. The Czech weather station data were provided by the Czech Hydrometeorological Institute.

References

Alley WM (1984) The Palmer Drought Severity Index: Limitations and assumptions. J Clim Appl Meteor 23:1100–1109.

Bonaccorso B, Bordi I, Cancelliere A, Rossi G, Sutera A (2003) Spatial Variability of drought: An analysis of the SPI in Sicily. Water Resour Man 17:273–296.

Bordi I, Sutera A (2001) Fifty years of precipitation: Some spatially remote teleconnections. Water Resour Man 15:247–280.

Brunetti M, Brunetti M, Maugeri M, Nanni T, Navarra A, Maugeri M, Nanni T, Navarra A (2002) Droughts and extreme events in regional daily Italian precipitation series. Int J Climatol 22:509–621.

Byun H-R, Wilhite DA (1999) Objective quantification of drought severity and duration. J Clim 12:2747–2756.

Dai A, Trenberth KE, Qian T (2004) A global dataset of Palmer Drought Severity Index for 1870–2002: Relationship with soil moisture and effects of surface warming. J Hydrometeor 5:1117–1130.

Dubrovsky M, Nemesova I, Kalvova J (2005) Uncertainties in climate change scenarios for the Czech Republic. Clim Res 29:139–156.

Guttman NB (1994) On the sensitivity of sample L moments to sample size. J Clim 7:1026–1029.

Guttman NB (1999) Accepting the Standardized Precipitation Index: A calculation algorithm. J Am Water Res Assoc 35:311–322.

Hayes MJ, Svoboda MD, Wilhite DA, Vanyarkho OV (1999) Monitoring the 1996 drought using the Standardized Precipitation Index. Bull Am Meteor Soc 80:429–438.

Heim RR (2002) A review of twentieth-century drought indices used in the United States. Bull Am Meteor Soc 83:1149–1165.

Hisdal H, Stahl K, Tallaksen LM, Demuth S (2001) Have streamflow droughts in Europe become more severe or frequent? Int J Climatol 21:317–333.

Houghton JT, Ding Y, Griggs DJ, Noguer M, van der Linden PJ, Xiaosu D (eds) (2001) Climate change 2001: The scientific basis. Contribution of Working Group I to the Third Assessment Report of the Intergovernmental Panel on Climate Change (IPCC). Cambridge University Press, Cambridge, p 944.

Huth R, Kysely J, Dubrovsky M (2001) Time structure of observed, GCM-simulated, downscaled, and stochastically generated daily temperature series. J Clim 14:4047–4061.

Jones PD, Hulme M, Briffa KR, Jones CG (1996) Summer moisture availability over Europe in the Hadley centre general circulation model based on the Palmer drought severity index. Int J Climatol 16:155–172.

Karl TR, Knight RW (1985) Atlas of monthly Palmer hydrological drought indices (1931–1983) for the contiguous United States. Historical climatology Series 3–7. National Climatic Data Center, Asheville, NC.

Keyantash J, Dracup JA (2002) The quantification of drought: An evaluation of the drought indices. Bull Am Meteor Soc 83:1167–1180.

Lana X, Serra C, Burgueno A (2001) Patterns of monthly rainfall shortage and excess in terms of the standardized precipitation index for Catalonia (NE Spain). Int J Climatol 21:1669–1691.

Lloyd-Hughes B, Saunders MA (2002) A drought climatology for Europe. Int J Climatol 22:1571–1592.

Martin-Vide J, Gomez L (1999) Regionalization of Peninsular Spain based on the length of dry spells. Int J Climatol 19:537–555.

McCarthy JJ, Canziani OF, Leary NA, Dokken DJ, White KS (eds) (2001) Climate change 2001: Impacts, adaptation & vulnerability. Contribution of Working Group II to the Third Assessment Report of the Intergovernmental Panel on Climate Change (IPCC). Cambridge University Press, Cambridge, p. 1000.

McKee TB, Doesken NJ, Kleist J (1993) Drought monitoring with multiple timescales. Preprints, Eighth Conf. on Applied Climatology, Anaheim, CA, Am Meteor. Soc., pp. 179–184.

Mitchell TD, Jones PD (2005) An improved method of constructing a database of monthly climate observations and associated high-resolution grids. Int J Climatol 25:693–712.

Oliver JE (ed) (2005) Encyclopedia of world climatology. Encyclopedia of Earth Sciences Series, Springer, Berlin Heidelberg New York, p 855.

Palmer WC (1965) Meteorological drought. Weather Bureau, Research Paper No. 45, U.S. Dept. of Commerce, Washington, DC, p 58.

Piccarreta M, Capolongo D, Boenzi F (2004) Trend analysis of precipitation and drought in Basilicata from 1923 to 2000 within a Southern Italy context. Int J Climatol 24:907–922.

Redmond KT (2002) The depiction of drought. Bull Am Meteor Soc 83:1145–1147.

Rouault M, Richard Y (2003) Intensity and spatial extension of drought in South Africa at different time scales. Water SA, vol 29, 489–500 [available free from http://www.wrc.org.za].

Seiler RA, Hayes M, Bressan L (2002) Using the standardized precipitation index for flood risk monitoring. Int J Climatol 22:1365–1376.

Smith JB, Huq S, Lenhart S, Mata LJ, Nemesova I, Toure S (1996) Vulnerability and adaptation to climate change: Interim results from the U.S. country studies program. Kluwer, Dordrecht, p 366.

Svoboda MD, LeComte D, Hayes MJ, Heim R, Gleason K, Angel J, Rippey B, Tinker R, Palecki M, Stooksbury D, Miskus D, Stevens D (2002) The drought monitor. Bull Am Meteor Soc 83:1181–1190.

Szalai S, Szinell C (2000) Statistical tests for drought tendency investigations and their sensitivity. In: Proc. 12th Conference on Applied Climatology, AMS, Boston, MA, pp 243–246.

Szinell CS, Bussay A, Szentimrey T (1998) Drought tendencies in Hungary. Int J Climatol 18:1479–1491.

Tolasz R, Mikova T, Valerianova A (eds) (2006) Climatic Atlas of Czechia, ČHMÚ (in press).

Tomasek M (200) Pudy Ceske republiky. CGU, Praha, p 67.

Touchan R, Funkhouser G, Hughes MK, Erkan N (2005) Standardized Precipitation Index Reconstructed from Turkish Tree-ring Widths. Clim Change 72:339–353.

Trnka M, Dubrovsky M, Svoboda MD, Semeradova D, Hayes MJ, Zalud Z, Wilhite DA (2008) Developing a regional drought climatology for the Czech Republic for 1961–2000. Submitted to Int J Climatol (August 06).

van der Schrier G, Briffa KR, Jones PD, Osborn TJ (2006) Summer moisture variability across Europe. J. Climate 19:2818–2834.

Vicente-Serrano SM, Beguería S (2003) Estimating extreme dry-spell risk in the middle Ebro valley (Northeastern Spain): A comparative analysis of partial duration series with a General Pareto distribution and annual maxima series with a Gumbel distribution. Int J Climatol 23:1103–1118.

Vicente-Serrano SM, González-Hidalgo JC, de Luis M, Raventós J (2004) Drought patterns in the Mediterranean area: The Valencia region (eastern Spain). Clim Res 26:5–15.

Watson RT, Zinyowera MC, Moss RH (eds) (1997) The regional impacts of climate change: An assessment of vulnerability. Cambridge University Press, Cambridge, p 517.

Wells N, Goddard S, Hayes MJ (2004) A self-calibrating Palmer Drought Severity Index. J Clim 17:2335–2351.

Wilhite DA (2000) Drought as a natural hazard: Concepts and definitions. In: Wilhite DA (ed) Drought: a global assessment, Routledge, pp 3–18.

Woodhouse CA, Brown PM (2001) Tree-ring evidence for Great Plains drought. Tree-Ring Res 59:89–103.

Woodhouse CA, Lukas JJ, Brown PM (2002) Drought in the Western Great Plains, 1845–56. Bull Am Meteor Soc 83:1485–1493.

Wu H, Hayes MJ, Wilhite DA, Svoboda MD (2005) The effect of the length of record on the standardized precipitation index calculation. Int J Climatol 25:505–520.

Zou X, Zhai P, Zhang Q (2005) Variations in droughts over China: 1951–2003. Geoph Res Lett 32:L04707.